Protein Science (1999), *8*:1990–2000. Cambridge University Press. Printed in the USA.

Three-dimensional structures of enzyme–substrate complexes of the hydroxynitrile lyase from *Hevea brasiliensis*

J. ZUEGG,[1,2,3,4] K. GRUBER,[1,4] M. GUGGANIG,[1,2] U.G. WAGNER,[1] AND C. KRATKY[1]

[1]Abteilung für Strukturbiologie, Institut für Physikalische Chemie, Karl-Franzens Universität Graz, Heinrichstrasse 28, A-8010 Graz, Austria
[2]Spezialforschungsbereich Biokatalyse, Technische Universität Graz, Stremayrgasse 16, A-8010 Graz, Austria

(RECEIVED March 17, 1999; ACCEPTED July 2, 1999)

Abstract

The 3D structures of complexes between the hydroxynitrile lyase from *Hevea brasiliensis (Hb*–HNL) and several substrate and/or inhibitor molecules, including trichloracetaldehyde, hexafluoracetone, acetone, and rhodanide, were determined by X-ray crystallography. The complex with trichloracetaldehyde showed a covalent linkage between the protein and the inhibitor, which had apparently resulted from nucleophilic attack of the catalytic Ser80-Oγ. All other complexes showed the substrate or inhibitor molecule merely hydrogen bonded to the protein. In addition, the native crystal structure of *Hb*–HNL was redetermined at cryo-temperature and at room temperature, eliminating previous uncertainties concerning residual electron density within the active site, and leading to the observation of two conserved water molecules. One of them was found to be conserved in all complex structures and appears to have mainly structural significance. The other water molecule is conserved in all structures except for the complex with rhodanide; it is hydrogen bonded to the imidazole of the catalytic His235 and appears to affect the *Hb*–HNL catalyzed reaction. The observed 3D structural data suggest implications for the enzyme mechanism. It appears that the enzyme-catalyzed cyanohydrin formation is unlikely to proceed via a hemiacetal or hemiketal intermediate covalently attached to the enzyme, despite the observation of such an intermediate for the complex with trichloracetaldehyde. Instead, the data are consistent with a mechanism where the incoming substrate is activated by hydrogen bonding with its carbonyl oxygen to the Ser80 and Thr11 hydroxy groups. A hydrogen cyanide molecule subsequently replaces a water molecule and is deprotonated presumably by the His235 base. Deprotonation is facilitated by the proximity of the positive charge of the Lys236 side chain.

Keywords: biocatalysis; cyanohydrin formation; enzyme mechanism; hydroxynitrile lyase; oxynitrilase; protein crystallography

Hydroxynitrile lyases (EC 4.2.1.39) catalyze the cleavage of cyanohydrins to yield hydrocyanic acid plus the corresponding aldehyde or ketone (Fig. 1). The release of HCN serves as a defense against herbivores and microbial attack for a variety of plants (Conn, 1981; Hickel et al., 1996; Wajant & Effenberger, 1996) and is initiated by a β-glycosidases–mediated degradation of cyanoglycosides, forming a sugar and the α-hydroxynitrile (cyanohydrin). In aqueous solution, cyanohydrin cleavage occurs spontaneously above pH 5, while the enzyme-catalyzed reaction also occurs at lower pH values (down to pH ~ 3; Hickel et al., 1996).

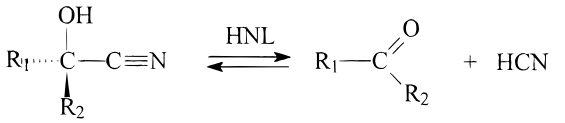

R_1 = alkyl or aryl, R_2 = CH_3 or H, $R_1 > R_2$

Fig. 1. The reaction catalyzed by hydroxynitrile lyase.

Reprint requests to: Christoph Kratky, Institut für Physikalische Chemie, Karl-Franzens Universität, Heinrichstrasse 28, A-8010 Graz, Austria; e-mail: christoph.kratky@kfunigraz.ac.at.

[3]Present address: J. Zuegg, John Curtin School of Medical Research, Australian National University, Department of Biochemistry and Molecular Biology, Canberra ACT 2612, Australia.

[4]These authors contributed equally to this work.

Abbreviations: 3D, three-dimensional; *Hb*–HNL, hydroxynitrile lyase from *Hevea brasiliensis*; HEPES, *N*-(2-hydroxy-ethyl)piperazine-*N*′-(2-ethanesulfonic acid); HNL, hydroxynitrile lyases; *Me*–HNL, hydroxynitrile lyase from *Manihot esculenta*; RMSD, root-mean-square deviation; TCA, trichloracetaldehyde; UV, ultraviolet.

Besides their biological interest, hydroxynitrile lyases (HNLs) are increasingly used as biocatalysts in the organic synthesis of chiral compounds (Kruse, 1992; Klempier et al., 1993; Johnson & Griengl, 1997, 1999), exploiting the reverse of the biological reaction, i.e., the stereospecific formation of cyanohydrins from HCN and an aldehyde or ketone. Chiral cyanohydrins are important synthetic intermediates for the production of a wide range of pharmaceuticals and agrochemicals (Effenberger, 1994).

HNLs have been isolated and purified from a large variety of plant species, and they have been classified into HNLs with and without an FAD cofactor (Hickel et al., 1996). FAD-dependent HNLs accept (*R*)(+)mandelonitrile as their biological substrate and appear to have evolved from FAD-dependent oxidoreductases (Kuroki & Conn, 1989). FAD-independent hydroxynitrile lyases accept a variety of (*R*) (Linacaeae; Xu et al., 1988) and (*S*) (Euphoribiacae; Hughes et al., 1994; Olacaeae; Kuroki & Conn, 1989; Graminae; Wajant & Mundry, 1993) configured cyanohydrins as substrates. The (*S*)-HNLs from *Manihot esculenta* (Euphoribiacae; Wajant & Pfizenmaier, 1996) and *Hevea brasiliensis* (Euphoribiacae; Hasslacher et al., 1996a, 1996b, 1997a; Wagner et al., 1996) belong to the α/β hydrolase superfamily. It appears that nature has invented oxynitrilases at least twice, once derived from FAD-dependent oxidoreductases, and once from α/β hydrolases (Ollis et al., 1992; Cygler et al., 1993).

The (*S*)-HNL from *H. brasiliensis* (*Hb*–HNL) is an unglycosylated protein with a subunit molecular mass of 29.2 kDa, which possibly occurs as a homodimer in neutral aqueous solution (Schall, 1996). The protein is highly homologous (76% sequence identity) to HNL from *M. esculenta* (Hasslacher et al., 1996a). Its natural substrate is acetone cyanohydrin, but in vitro it accepts a variety of aliphatic, aromatic, and heterocyclic aldehydes or ketones for the (*S*)-specific synthesis of the corresponding α-cyanohydrins (Klempier et al., 1993, 1995; Johnson & Griengl, 1997). Its 3D structure (Fig. 2; Wagner et al., 1996) unequivocally established the enzyme to belong to the α/β hydrolase fold family.

Based on the well-established mechanism of serine hydrolases (Wharton, 1998), a reaction mechanism was suggested for the *Hb*–HNL (Wagner et al., 1996), which postulated a hemiacetal or hemiketal intermediate resulting from nucleophilic attack of the active site serine oxygen on the substrate's carbonyl group. An alternative reaction mechanism with general acid/base catalysis was suggested from site-directed mutagenesis experiments (Wajant & Pfizenmaier, 1996) for the homologous enzyme from *M. esculenta* (*Me*–HNL).

Here, we report the preparation and crystallographic structure elucidation of complexes between *Hb*–HNL and several substrates and inhibitors. The objective of our studies was the structural characterization of potential reaction intermediates, which should lead to an experimental elucidation of the molecular mechanism of enzyme-catalyzed cyanohydrin formation or cleavage.

Results

The native crystal structure of *Hb*–HNL was redetermined from enzyme preparations purified with TRIS buffer (see below) at room temperature and at cryo-temperature. Crystals of *Hb*–HNL complexes were prepared by soaking (typically for several hours) native crystals in their mother liquor containing the substrate/inhibitor in millimolar concentrations (see Table 1 for details). All crystals investigated were found to be more or less isomorphous (space group $C222_1$ with very similar cell parameters, see Table 1)

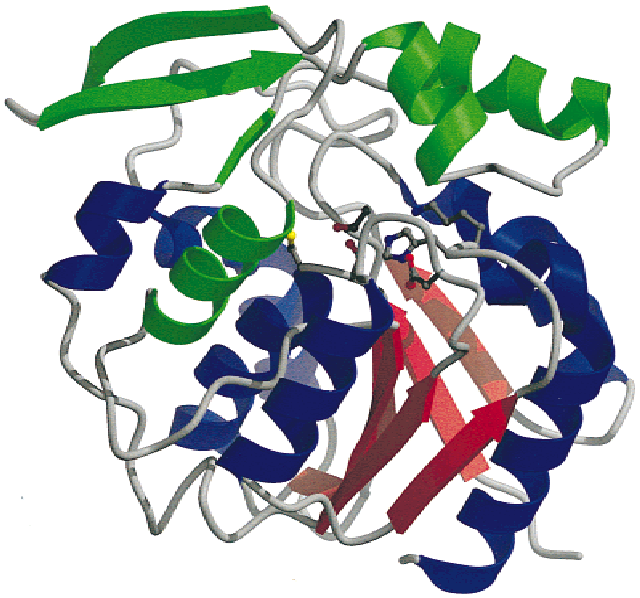

Fig. 2. Ribbons representation (programs MOLSCRIPT, Kraulis, 1991; and Raster3D, Merritt & Bacon, 1997) of the 3D structure of *Hb*–HNL, with the following active-site residues shown: Thr11, Ser80, Cys81, Asp207, His235, and Lys236.

to the crystals used for the original analysis of the native *Hb*–HNL structure (Wagner et al., 1996). The structures were refined against diffraction data extending to between 2.3 and 1.7 Å (see Table 1).

The native structure

The original analysis of the native *Hb*–HNL crystal structure (Wagner et al., 1996) had revealed residual electron density within the active site, which was tentatively assigned to a histidine molecule. Presumably, this molecule had been picked up during the purification from the histidine sulfate buffer. Because the chemical constitution of the bound inhibitor was not unambiguous, we have redetermined the native *Hb*–HNL structure from a crystal obtained from a preparation purified in Tris buffer (instead of the originally used histidine buffer). A first analysis, performed at cryo-temperature from synchrotron data to 1.75 Å resolution, still showed poorly defined residual density within the active site (see Fig. 3B); while two density features can reasonably be assigned to water molecules, the remaining density is more difficult to interpret and might either originate from additional disordered water molecules or from a disordered glycerol molecule used as cryoprotectant. In all cryo-temperature diffraction experiments, crystals were briefly (several seconds) soaked in a solution containing *a* high (30% v/v) concentrations of glycerol. Despite the short soaking time, observation of protein-attached cryoprotectant molecules are not unprecedented (Schmidt et al., 1998, 1999).

Because the disordered density was located near the binding site of some of the substrate or inhibitor molecules, we collected a second native data set at room temperature from a crystal mounted in a capillary without cryoprotectant. This time, the residual density (Fig. 3A) is readily interpretable as originating from three water molecules. A fully conserved "structural" water molecule (Wat501) is hydrogen bonded to the His235 main-chain carbonyl

Table 1. *Summary of kinetic and crystallographic data*

	nat-lt[a]	nat-rt[a]	Acetone	F_6-acetone	TCA[a]	Rhodanide
Inhibition constant			30 mM	0.55 mM	0.39 mM	5.5 μM[b]
Soaking concentration			400 mM	25 mM	5 mM	1 mM
Data collection temperature	110 K	300 K	95 K	95 K	110 K	105 K
X-ray source[c]	Elettra 5.2	Home	EMBL X31	EMBL X31	Elettra 5.2	EMBL X11
Cell parameters						
a (Å)	47.5	47.6	47.5	47.5	47.6	47.4
b (Å)	106.4	109.1	106.7	106.4	106.8	106.8
c (Å)	128.4	128.6	128.1	128.2	128.2	128.8
Used resolution range	28–1.75	10–2.20	16–1.85	16–2.00	15–2.00	14–1.72
Inner shell	28–6.60	10–5.81	16–5.53	16–5.92	15–6.93	14–4.62
Outer shell	1.81–1.75	2.31–2.20	1.95–1.85	2.11–2.00	2.07–2.00	1.75–1.72
R_{Merge} (%) overall/outer shell	3.7/11.3	5.0/13.2	9.1/29.0	10.2/28.3	9.2/11.3	6.6/23.7
$\langle I/\sigma(I)\rangle$ overall/outer shell	16.0/6.6	12.2/5.6	7.6/2.6	5.3/2.7	6.7/6.3	18.9/5.8
Data completeness (%)	91.6	84.5	99.0	98.4	93.6	98.7
Inner shell/outer shell	97.9/97.8	75.2/88.3	100/99.0	98.3/96.9	100/100	94.8/99.6
Number of unique reflections	30,389	14,339	27,904	21,969	21,088	34,663
Redundancy	4.1	4.2	3.9	3.4	7.6	3.8
R/R_{free} (%)	19.1/21.8	15.9/22.1	19.0/22.7	18.7/24.1	18.7/22.1	15.0/19.1
Number of H_2O/SO_4 molecules	302/3[d]	124/1	336/4	342/4	318/3	335/4
Backbone RMSD to 1YAS (Å)	0.21	0.15	0.23	0.23	0.19	0.21
PDB entry code	7YAS	6YAS	3YAS	5YAS	4YAS	2YAS

[a] nat-lt and nat-rt denote the low- and room-temperature native data; TCA denotes trichloracetaldehyde.
[b] Data from reference (Schall, 1996, p. 173).
[c] See Materials and methods for more details of the beam lines.
[d] In addition, one glycerol and one HEPES molecule were observed.

oxygen and the side chains of Glu79 and His103. A second "central" water molecule (Wat500) is suspended between the His235 and Lys236 side chains. This water molecule is conserved in many—although not all—substrate/inhibitor complexes and is suggested to be significant for the enzyme mechanism. A third "active-site" water molecule (Wat502) is located near the Thr11 and Ser80 side chains and hydrogen bonds to the "central" water molecule Wat500. The "active-site" water is invariably replaced by substrate or inhibitor molecules binding to the active site, and it was only observed in the native room-temperature structure.

Enzyme inhibitor complexes

Trichloracetaldehyde

Refinement against synchrotron data to a resolution of 2.0 Å, collected from a crystal soaked in 5 mM (see Table 1) trichloracetaldehyde (TCA) yielded residual electron density within the active site cavity, some of which unambiguously originated from a molecule of trichloracetaldehyde covalently attached to Oγ of Ser80 (see Fig. 4). Evidently, this tetrahedral adduct is the result of a nucleophilic attack of the Ser80-Oγ on the *Re*-face of a TCA molecule, leading to a hemiacetal of stereochemical (*R*) configuration. The hydroxyl oxygen atom of the hemiacetal is located near the position occupied by the "central" Wat500 in the native structure. Wat500 appears to have shifted toward Wat501, to which it is now connected by a hydrogen bond. Its large *B*-factors (about twice the values of the active site residues) indicate less-than-full occupancy of the hemiacetal. Moreover, weak residual density is still visible at the location occupied by Wat500 in the native structure (about 1.7 Å away from the hemiacetal-OH).

Disordered residual density was also observed near Cys81, likely to originate from a second partially occupied TCA molecule, possibly attached to the Cys81-Sγ (Fig. 4B). However, attempts to model this density by a TCA molecule in a single conformation led to unsatisfactory results. In fact, steric considerations suggest that the Cys81-Sγ and the Ser80-Oγ cannot be simultaneously occupied by a covalently attached TCA molecule, which is in line with incomplete occupancy at this site. It thus appears that the two sites—near Ser80 and near Cys81—are both partially occupied, with the occupancy of the Ser80-site predominating.

Hexafluoracetone

Like trichloracetaldehyde, hexafluoracetone is predominantly hydrated in aqueous solution, i.e., it occurs as the corresponding gem-diol. It is a strong inhibitor of *Hb*–HNL (see Table 1), and soaking experiments with subsequent structure analysis revealed substantial residual electron density within the active site. Because there is no contiguous density to the Ser80-Oγ (Fig. 5A), formation of a covalently attached hemiketal can be excluded for this inhibitor.

As in solution, the inhibitor occurs in the crystal as gem-diol. One of its hydroxyls is suspended between the OH groups of Thr11 and Ser80 and the water molecule Wat500. The second ketal-OH is not involved in any H-bonds; the nearest neighbors are the backbone carbonyl group of Ile12 (3.4 Å) and the Nϵ atom of His14 (3.6 Å). Refinement of the model shown in Figure 5A led to *B*-factors around 30 Å^2, which contrasts with values around 10 Å^2 for the protein active site residues. The two water molecules Wat500 and Wat501 occupy approximately the same positions as in the native structure.

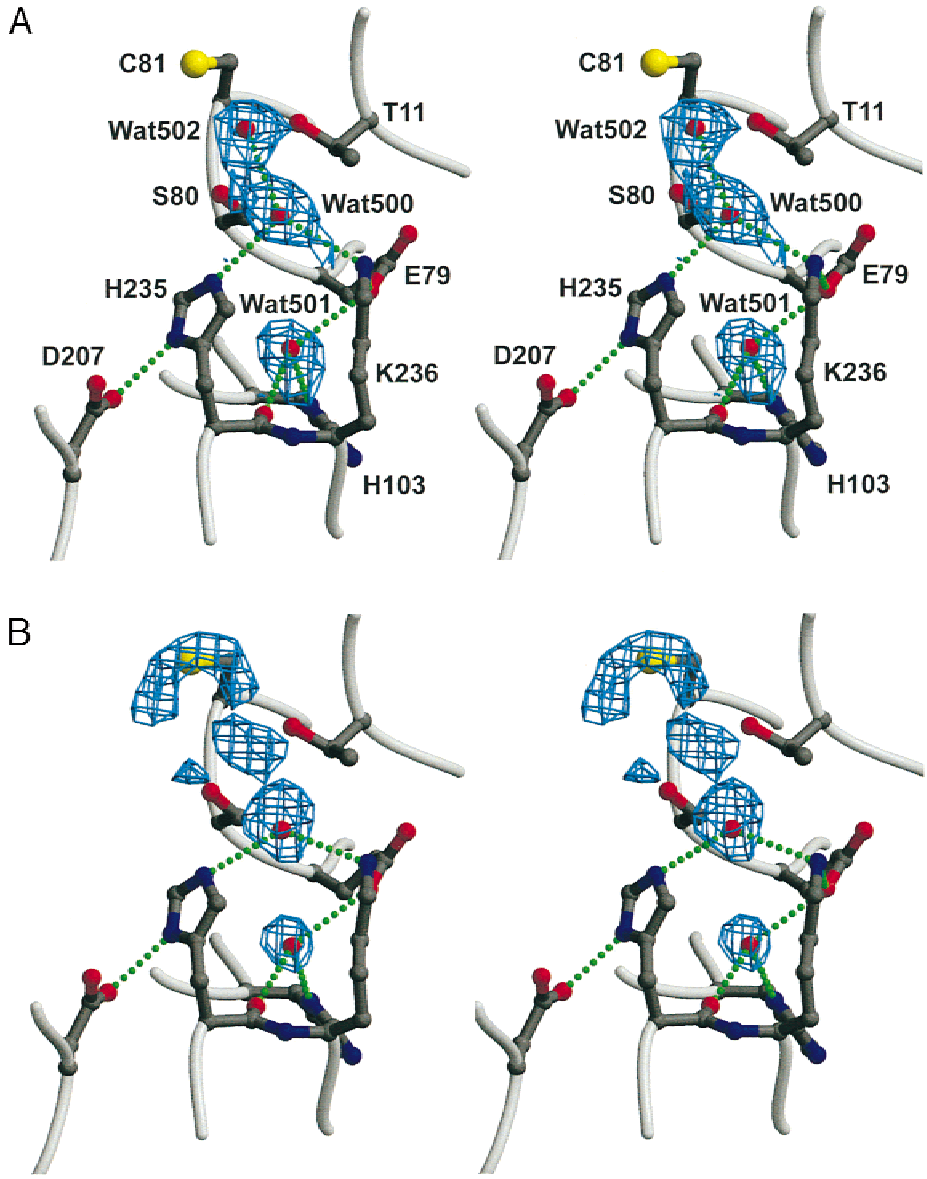

Fig. 3. Stereoview of the active site of HNL. C-, N-, O-, and S-atoms are depicted as gray, blue, red, and yellow spheres, respectively; halogens are light green. Hydrogen bonding interactions ($d < 3.2$ Å for bonds involving only nitrogen and oxygen, $d < 3.3$ Å for interactions involving also sulfur) are represented by dotted lines. For the residual density within the active site, σ_A-weighted (Read, 1986) $3F_o - 2F_c$ Bhat-omit maps (Bhat & Cohen, 1984; Bhat, 1988; Vellieux & Dijkstra, 1997) were computed and are shown at a 1.5σ contour level. The phases used for generating these maps were calculated from the final protein coordinates after adding random positional errors that yielded an RMSD of 0.25 Å. Figures prepared with programs MOLSCRIPT (Kraulis, 1991) and Raster3D (Merritt & Bacon, 1997). (**A**) Native density computed from data collected at room temperature (nat-rt); (**B**) low-temperature native structure (nat-lt).

The corresponding density for a crystal soaked in Cl_6-acetone (data not shown) was more problematic due to extensive disorder, but yielded essentially the same picture. Although the gross features appeared at roughly the same location as for F_6-acetone, only one of the two trichloromethyl groups could be assigned with confidence.

Rhodanide

The structure was refined against synchrotron diffraction extending to 1.72 Å resolution. As with the other inhibitors, the conformation of the polypeptide changed little upon rhodanide binding. Clear density appeared within the active site (Fig. 5B), readily assignable to a rhodanide ion. Its *B*-factors (Table 2) indicate a reasonable occupancy of the ligand. Within the ion, the *B*-factors are more or less uniform (S: 24 Å^2, C: 17 Å^2, and N: 18 Å^2). Interconversion of S and N resulted in *B*-factors of 33 Å^2 for S and 8 Å^2 for N.

The nitrogen atom of SCN is found at the position of the "central" water molecule Wat500, where it interacts with His235 and Lys236. The sulfur atom is in hydrogen-bonding distance to the side-chain oxygen atoms of Ser80 and Thr11. Only minor conformational changes with respect to the native *Hb*–HNL structure had

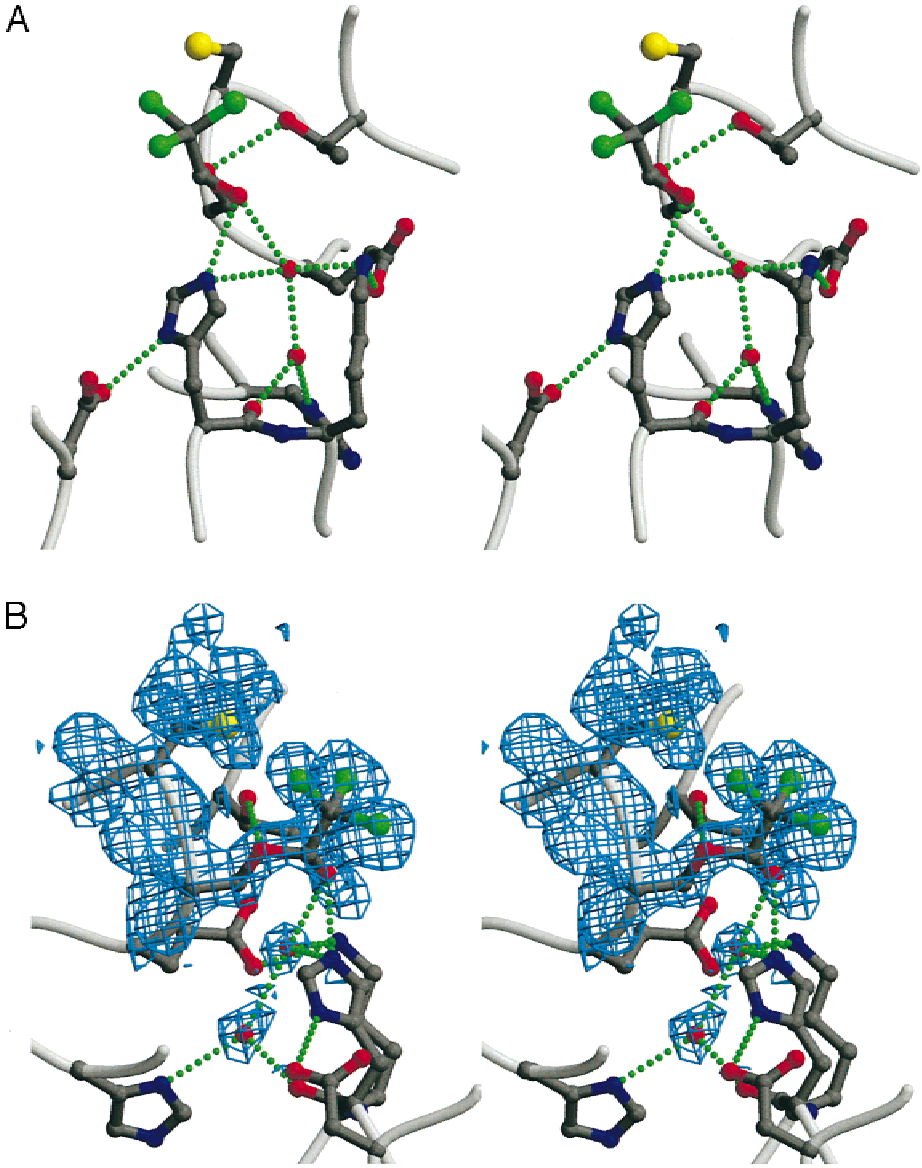

Fig. 4. (**A**) Structure and (**B**) observed residual density of the complex between *Hb*–HNL and trichloracetaldehyde. The view shown in **B** is related to the one of **A** by a 90° rotation about a vertical axis. See caption to Figure 3 for details.

occurred within the active site. Notably, Ser80 moved toward His235, leading to the shortest distance between these two residues observed so far (Table 2).

Acetone

The refined model after soaking with the biological reaction product revealed clear residual electron density readily interpretable as a hydrogen bonded—but not covalently attached—acetone molecule. In fact, the relatively low *B*-factors of its atoms (Table 2) indicate full occupancy. The carbonyl oxygen of the acetone molecule is involved in hydrogen bonds to the OH groups of Ser80 and Thr11 (Table 2; Fig. 5C). Its two methyl groups are located in a hydrophobic region of the active site, where they are surrounded by residues Leu142, Ile12, Leu157, Trp128, and Ile209. The two water molecules (Wat500 and Wat501) are well defined and refined to similar *B*-values as the acetone. The position of Wat500 is remarkable (Fig. 5C): while it forms hydrogen bonds to His235 and Lys236, it is also quite close to the acetone molecule, with distances of 3.25 Å to the carbonyl carbon and 3.45 Å to the carbonyl oxygen. Geometrically, it appears to be ideally positioned for nucleophilic attack on the carbonyl group (Bürgi et al., 1973). In fact, the exact locations of the protons for this water molecule are not obvious and depend on the protonation state of the His235 and Lys236 side chains: while Wat500 is likely to act as a hydrogen bond donor to the His235-Nϵ, it has to accept a H-bond from Lys236 if the latter is present in the protonated form. Considering that one of the water molecule's lone pairs is involved in a donor–acceptor interaction with the (electrophilic) carbonyl carbon, the second proton has to point toward a hydrophobic pocket consisting of Leu148 and Leu157. Alternatively, in order for Lys236 to be

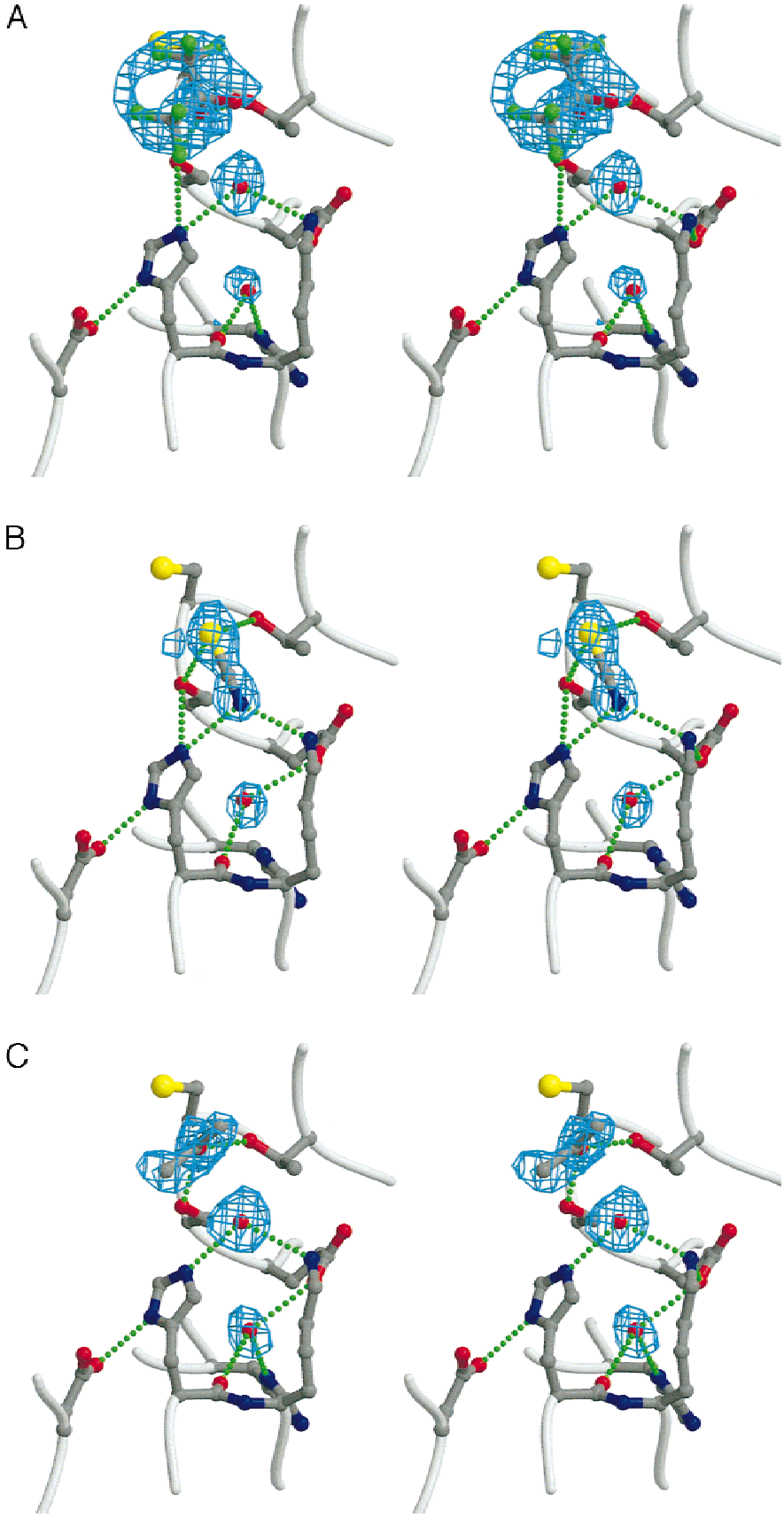

Fig. 5. Residual density within the active site of *Hb*–HNL for the (**A**) F_6-acetone, (**B**) rhodanide, and (**C**) acetone soaks. See caption to Figure 3 for details.

Table 2. *Structural results*

	nat-lt	nat-rt	Acetone	F_6-acetone	TCA	Rhodanide
⟨*B*(overall)⟩ (Å^2)[a]	8.3	19.3	6.9	6.4	6.4	19.5
⟨B(Substr./Inh.)⟩ (Å^2)			12.8	32.7	20.8	19.8
Distance Ser80.Oγ—His235.Nϵ2	3.36	3.30	3.20	3.16	4.05	2.98
Distance Wtr500—Ser80.Oγ	3.67	3.30	3.54	3.48	4.07	
Distance Wtr500—His235.Nϵ2	2.87	3.11	2.87	2.94	2.93	
Distance Wtr500—Lys236.Nζ		2.87	3.05	2.98	2.90	2.81
Distance Wtr500—Wtr501	4.93	5.45	5.34	5.00	3.11	
Distance substrate/inhibitor—Ser80.Oγ			2.65[b]	2.55[c]		3.20[d]
Distance substrate/inhibitor—Thr11.Oγ			2.78[b]	2.88[c]	3.74[e]	3.26[d]
Distance substrate/inhibitor—Wtr500			3.45[b]	3.26[c]	2.94[e]	
Distance substrate/inhibitor—Lys236.Nζ			5.94[b]	5.78[c]	4.46[e]	2.90[f]
Distance substrate/inhibitor—His235.Nϵ2			4.72[b]	4.59[c]	2.82[e]	3.02[f]

[a] Average *B*-factor for all protein atoms.
[b] Distance from carbonly oxygen.
[c] Distance from one of the OH groups of F_6-acetone hydrate.
[d] Distance from the sulfur atom.
[e] Distance from hemiacetal OH.
[f] Distance from the nitrogen atom.

able to accept a hydrogen bond from Wat500, one has to assume its side chain to occur as the unprotonated amine, which is disputable in view of the proximity of Glu79.

Discussion

Active site geometry

The 3D structure of the hydroxynitrile lyase from *H. brasiliensis* (Wagner et al., 1996) confirmed this enzyme to belong to the α/β hydrolase superfamily (Fig. 2). Amino acid sequence alignment also suggests the same fold for the homologous enzyme from *M. esculenta* (*Me*–HNL). Characteristic features of the α/β hydrolase fold are an extended parallel β-sheet flanked on both sides by α-helices, as well as a catalytic triad consisting of three conserved residues (Ser,His,Asp/Glu) in topologically and structurally related loop regions. Functionally, the serine oxygen acts as a nucleophile, activated by a chain of hydrogen bonds involving the histidine–imidazole and the carboxylate of the acid residue. The correct geometry of this triad is believed to be essential for the proteolytic activity of serine hydrolases (Barth et al., 1994), with special relevance for a short distance between the three residues (Wallace et al., 1996). For the HNL of *H. brasiliensis*, the triad consists of residues Ser80, His235, and Asp207. Although the enzyme shows no hydrolase activity, mutagenesis data indicate at least two of the three residues (Ser80 and His235) to be essential for the cyanogenic activity of HNL (Wajant & Pfizenmaier, 1996; Hasslacher et al., 1997a).

In the native structure, the active site cavity is occupied by several water molecules (Fig. 3A), one of which (Wat501) is conserved in all structures analyzed, the other one (Wat500) in all but the rhodanide complex. The presence of water molecule Wat500, which competes with the Ser80-Oγ as H-bonding partner of His235-Nϵ, consistently leads to an elongation of the direct hydrogen bond between Ser80 and His235 (Table 2), which decreases the basicity of Ser80.

A similar water molecule was observed in the "closed" and presumably inactive conformation of two lipases belonging to the α/β hydrolase superfamily, from *Geotrichum candidum* (Protein Data Bank (PDB) entry code 1thg; Schrag & Cygler, 1993) and from *Candida rugosa* (1trh; Grochulski et al., 1994). The corresponding open and active form of the *C. rugosa* enzyme (1crl; Grochulski et al., 1993) lacks the water molecule within the catalytic triad.

Two enzyme mechanisms were proposed for the two closely related (*S*)-hydroxynitrile lyases from *H. brasiliensis* (*Hb*–HNL) and *M. esculenta* (*Me*–HNL). In analogy to the mechanism of serine hydrolases, it was suggested (Wagner et al., 1996) that Ser80 would act as a nucleophile attacking (in the synthesis direction) the carbonyl group of the substrate ketone or aldehyde to form a covalently attached hemiketal or hemiacetal intermediate. Formation of this intermediate was suggested to be facilitated by an oxyanion hole formed by the main-chain NH of Cys81 and the side chains of Cys81 and Thr11. The step following hemiacetal or hemiketal formation would consist of nucleophilic substitution of the Ser80 oxygen by a cyanide ion. In contrast, an alternative mechanism devoid of a covalent enzyme–substrate intermediate was proposed, which suggests general acid-base catalysis involving the histidine and serine residues of the catalytic triad (Wajant & Pfizenmaier, 1996).

We have prepared several enzyme–substrate and enzyme–inhibitor complexes using substrate/inhibitor concentrations exceeding by at least one order of magnitude the corresponding K_M or K_I (Table 1). Insofar as these inhibitors mimic one of the substrates, the observed structures can be considered as models for the Michaelis complex. Evidently, the natural reaction product acetone is of particular relevance, as would be the structure of the complex with the biological substrate acetone cyanohydrin. However, attempts to prepare the latter complex failed so far, most probably due to its rapid cleavage under the soaking conditions. Likewise, attempts to observe the structure of *Hb*–HNL complexed with members of the mandelonitrile/benzaldehyde pair were unsuccessful, possibly as a result of the limited solubility of these compounds in the (aqueous) crystallization solutions.

At first sight, the 3D structures of the above complexes appear somewhat contradictory: complexes with a covalent connection between inhibitor and enzyme (trichloracetaldehyde) were observed as well as complexes where the inhibitor or substrate is only hydrogen bonded to the protein (e.g., acetone). However, closer scrutiny of the structures relieve some of this ambiguity.

A covalent intermediate . . .

Appraisal of the TCA–HNL complex (Fig. 4) as a model for the catalytic intermediate has to include the observed stereoselectivity of the *H. brasiliensis* HNL, which specifically cleaves (or forms) the (*S*)-enatiomer of the model substrate (or product) mandelonitrile. S_N2-type substitution of the Ser80-oxygen by a cyanide ion in the TCA–HNL complex would lead to (*S*)-trichloracetaldehyde-cyanohydrin (which would then be immediately hydrolyzed in aqueous solution). It is reasonable to assume that a corresponding covalent intermediate for the reaction with benzaldehyde would have the phenyl group oriented approximately in the direction of the TCA complex's trichloromethyl group. This would—as a result of the changed sequence of priorities for the Cahn-Ingold-Prelog nomenclature (Prelog, 1964)—then yield (*R*)-mandelonitrile, at variance with the experimental stereoselectivity of *Hb*–HNL. Thus, the observed covalent TCA–HNL complex appears to be a poor model for a catalytic intermediate of the HNL catalyzed reaction, giving no support to a mechanism involving such an intermediate.

. . . or one that is only hydrogen bonded?

Acetonecyanohydrin is the natural substrate of the hydroxynitrile lyase from *H. brasiliensis*, and the observed structure of the *Hb*–HNL complex with acetone is, therefore, likely to represent *some* intermediate along the reaction path. Although the lack of observation of a covalent linkage between the enzyme and the product does not unequivocally disprove the occurrence of such an intermediate along the reaction path, it makes it rather unlikely. Kinetic data (Bauer et al., 1999) for the cleavage and synthesis of mandelonitrile show the enzyme to follow a sequential uni-bi mechanism, with (in the synthesis direction) benzaldehyde binding first to HNL and cyanide only binding to the HNL–benzaldehyde complex. It is very likely that a similar mechanism also applies to the acetone–cyanohydrin formation. Thus, the complex observed under saturating acetone concentrations is likely to represent the first Michaelis complex for the HNL catalyzed synthesis of acetone–cyanohydrin.

Attack of cyanide

For the synthesis reaction, the step following formation of the Michaelis complex between HNL and acetone is the attack of cyanide on the substrate, which is activated as a result of hydrogen bonds between its carbonyl oxygen and the OH groups of Ser80 and Thr11 (Fig. 5C). Because cyanide occurs predominantly as the protonated (and unreactive) hydrocyanic acid under mildly acidic conditions ($pK_a \sim 9.3$), the nucleophilic attack has to follow deprotonation of HCN. This raises the question for the deprotonating base. A second question concerns the direction of nucleophilic attack, i.e., whether CN^- attacks the side of the substrate facing Cys81 or the opposite one, facing Wat500 (Fig. 5C).

Rhodanide acts as a very strong competitive inhibitor for *Hb*–HNL (Schall, 1996). Its structure shows that the rhodanide ion has replaced the otherwise conserved water molecule Wat500 (Fig. 5B), and that its presence decreases the distance between Ser80 and His235 (Table 2). It is tempting to hypothesize that the cyanide ion has its binding site near the "nitrogen end" of the *Hb*–HNL bound rhodanide, i.e., approximately at the position occupied otherwise by the "central" water molecule Wat500. CN^- would then be ideally positioned for nucleophilic attack on the substrate carbonyl, and the proximity of the (presumably) positive charges of His235 and Lys236 will decrease the pK_a of HCN via stabilizing the negatively charged CN^-. Along the same line of arguments, nucleophilic attack of CN^- from the opposite side would be disfavored by the water molecule Wat500. The structure of the complex with hexafluoracetone hydrate can be regarded as a very crude model for the complex with acetone cyanohydrin, if one imagines that one of its hydroxy groups is replaced by a nitrile. Although one OH group hydrogen bonds to the Ser80-Oγ and Thr11-Oγ, the other one points roughly in the direction of Wat500.

We have to note, however, that the channel connecting the active site with the protein exterior runs past the Cys81 side chain, i.e., toward the top of the page for the orientation shown in Figure 5. Consequently, access to the Wat500 site from the protein exteriour through this tunnel is congested once the substrate is bound. Thus, for the synthesis reaction, CN^- either has to bind before the substrate, which is at variance with kinetic evidence (Bauer et al., 1999), or it has to diffuse past the bound substrate to replace the water molecule Wat500, which would simultaneously have to diffuse out along the reverse route.

Mechanism of the enzyme-catalyzed cyanohydrin formation

The schematic representation of a mechanism for the HNL catalyzed cleavage or synthesis of acetone cyanohydrin consistent with the experimental evidence is presented in Figure 6. Key aspects of this mechanism are (for the cyanohydrin synthesis direction): (1) binding and activation of the substrate ketone or aldehyde by residues Ser80, Thr11, and possibly Cys81; (2) replacement of Wat500 by the incoming HCN, whose pK_a is decreased by the positively charged Lys236, and which is deprotonated by His235; (3) nucleophilic attack of CN^- on the substrate to yield the product cyanohydrin. For the cleavage direction, the reaction steps are analogous in the reverse direction. Although this mechanism is similar to a mechanism proposed previously for the *Me*–HNL enzyme (Wajant & Pfizenmaier, 1996), it differs with respect to the identification of residues involved in interactions with the substrate (apart from Ser80 also Thr11 and possibly Cys81), and with regard to the recognition of the importance of the Wat500 site and the Lys236 charge.

Hydroxynitrile lyase thus constitutes an enzyme with α/β hydrolase fold and with the full catalytic machinery of a serine hydrolase. Contrary to serine hydrolases, however, its mechanism does not appear to involve a tetrahedral intermediate, resulting from nucleophilic attack of the activated serine residue on the substrate's carbonyl group. However, although analogy with simple chemical reactions supports such a tetrahedral intermediate for the acylation and deacylation steps of serine hydrolases (Wharton, 1998), no direct evidence has so far been obtained to verify its existence. Notably, the mechanisms proposed for cystein hydrolases (Menard et al., 1990) and for phospholipase A2 (discussed in Quinn & Feaster, 1998) are somewhat similar to the suggested HNL mechanism: in the latter case, Nδ of His48 acts as a general base that deprotonates a water molecule to activate it for nucleophilic attack on the substrate carbonyl.

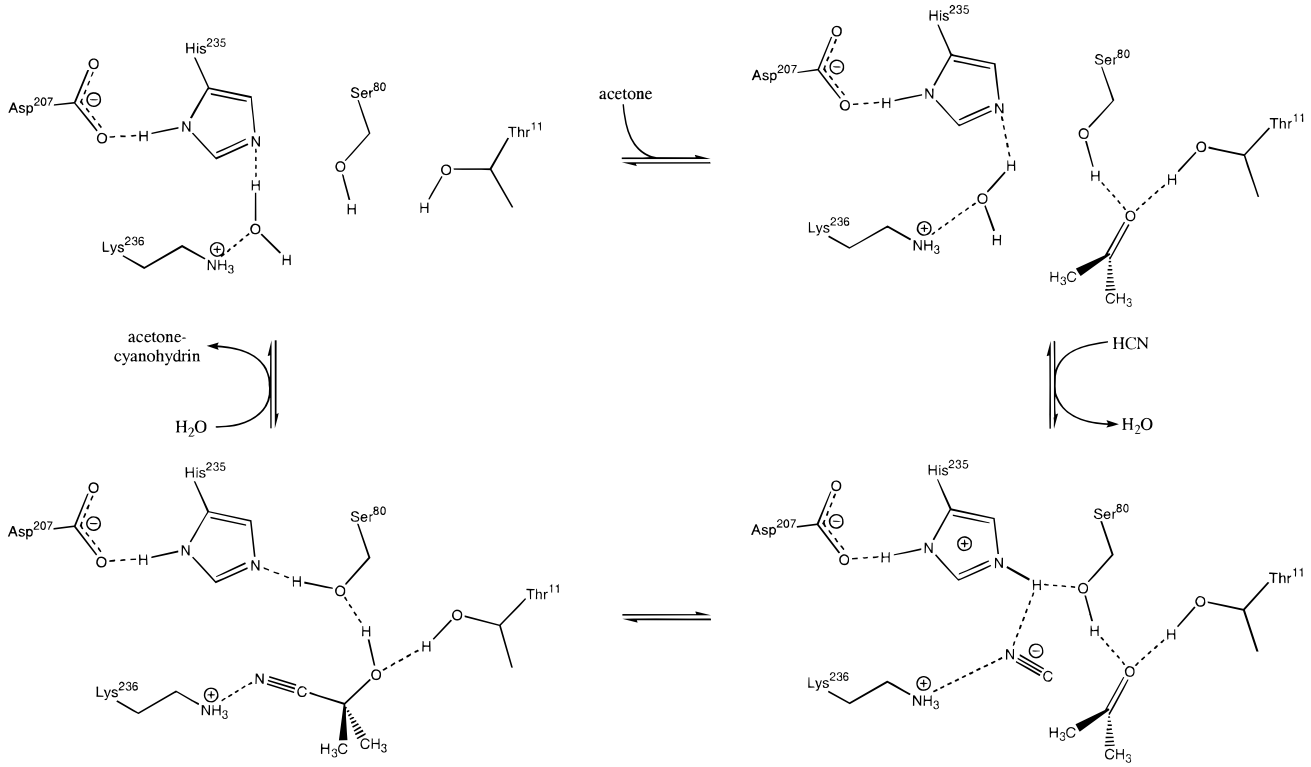

Fig. 6. Schematic representation of the steps involved in the *Hb*–HNL catalyzed reaction.

Materials and methods

Enzyme preparation and crystallization

Recombinant hydroxynitrile lyase from *H. brasiliensis* was overexpressed from *Pichia pastoris* (yeast; Hasslacher et al., 1997b) and purified to homogeneity as described previously (Wagner et al., 1996; Hasslacher et al., 1997a). The first step of the purification protocol consists of ion exchange chromatography of the crude extract on a Resource Q column (Pharmacia Biotech, Uppsala, Sweden). The HNL was eluted with a linear salt gradient increasing from 0 to 0.6 M $(NH_4)_2SO_4$ in 10 mM Tris-buffer [tris(hydroxymethyl)amino-methane)] pH 6.7. The second step consists of a size exclusion chromatography on a Superrose 12 column, equilibrated with 100 mM potassium phosphate, at pH 6.5 (Hasslacher et al., 1996a). Using the hanging drop vapor diffusion method, crystals were grown from 2% PEG 400 (polyethylenglycol), 2.0 M ammonium sulfate in 0.1 M Na HEPES buffer (2-[4-(2-hydroxyethyl)-1-piperazino]-propanesulfanic acid) at pH 7.5. In some preparations, crystals could also be obtained from preparations that had the size-exclusion chromatographic step omitted.

Crystalline enzyme–inhibitor or enzyme–substrate complexes were prepared by putting crystals of HNL into reservoir solution containing the corresponding inhibitor or substrate. Soaking times varied between 5 and 17 h. The inhibitors hexafluoracetone and trichloracetaldehyde were purchased from Aldrich as the corresponding hydrates.

Data collection and processing

Diffraction data sets of enzyme–inhibitor and enzyme–substrate complexes were all collected at cryogenic temperature (Table 1). Before flash freezing, crystals were soaked for about 5–10 s in a cryoprotectant, consisting of the reservoir solution with inhibitor or substrate, plus 30% glycerol. From this cryoprotectant, crystals were picked up with a fiber loop and dumped into liquid nitrogen. In addition to the complexes, two data sets were collected from native crystals without substrate or inhibitor, i.e., one low-temperature and one room-temperature data set, the latter with the crystal mounted in a capillary without cryoprotectant.

Diffraction data were collected at the EMBL beamlines X31 (equipped with a MAR-300 imaging plate detector) and X11 (MAR-345 detector) at Hasylab (DESY, Hamburg, Germany), at the crystallographic beamline 5.2 R at ELETTRA (Trieste, Italy; MAR-180 detector) and on a Siemens rotating anode generator (operated at 40 kV and 80 mA, graphite monochromator, MAR-300 detector). The data reduction involved the programs DENZO and SCALEPACK (Otwinowski, 1990) as well as programs from the CCP4 suite (CCP4, 1994).

Model building and refinement

All structures are isomorphous to the published crystal structure of *Hb*–HNL (PDB code 1yas; Wagner et al., 1996), whose coordinates were used as starting point for the refinement with X-PLOR (Brünger, 1992b) and SHELXL-97 (used only for the rhodanide data, where refinement was against F2 quantities using parameters, as described in Sheldrick, 1997; Gruber et al., 1998). All model building and fitting steps involved the graphic program O (Jones et al., 1991), using σ_A weighted $2F_o - F_c$ and $F_o - F_c$ maps (Read, 1986). Data collection and refinement statistics are shown in Table 1. The R_{free} values (Brünger, 1992a) were computed from 5–10% randomly chosen reflections not used for the refinement.

RMS deviations from ideal values ranged between 0.01 and 0.015 Å for bond lengths, between 2 and 3° for bond angles, and between 20 and 26° for dihedrals. A Ramachandran plot (performed with PROCHECK; Laskowski et al., 1993) showed all residues in all structures in core or allowed regions, with the exception of residues Ser80 and Lys129, which were always observed in disallowed regions of ϕ/ψ space. Although Ser80 is known to occur in a somewhat strained conformation in α/β hydrolases (Ollis et al., 1992), the density of Lys129 was found to be well defined throughout.

Kinetic studies

Enzyme kinetic experiments were performed to investigate the inhibition constants of several inhibitors. These studies were based on the degradation reaction of racemic mandelonitrile by the HNL, monitoring the formation of benzaldehyde by UV spectroscopy at a wavelength of 280 nm (Gugganig, 1997; Bauer, 1998). The enzyme concentration was also determined UV-spectroscopically at 280 nm (extinction coefficient of 27,386 AU M^{-1} cm^{-1} taken from Bauer, 1998). All kinetic investigations were carried out in 20 mM glutamate buffer at pH 5.0, and included the subtraction of the nonenzymatic base-catalyzed background reaction, which was typically slower by one order of magnitude than the enzyme-catalyzed reaction (Gugganig, 1997).

Acknowledgments

We acknowledge the financial support from the Österreichischer Fonds zur Förderung der wissenschaftlichen Forschung through the Spezialforschungsbereich Biokatalyse, as well as through project 11599. Synchrotron data were collected at the EMBL beamlines X31 and X11 at DESY in Hamburg, Germany and at beamline 5.2 R at the ELETTRA Synchrotron Light Source in Trieste, Italy. We thank H. Schwab and K. Rumbold for supplying purified protein, H. Griengl, W. Steiner, and M. Bauer for stimulating discussions on the enzymic mechanism.

References

Barth A, Forst K, Wahab M, Brandt W, Schlader HD, Franke R. 1994. Classification of serine proteases derived from steric comparisons of their active site geometry, part II: Ser, His, Asp arrangements in proteolytic and non-proteolytic proteins. *Drug Design Discovery 12*:89–111.

Bauer M. 1998. Kinetic investigation of the hydroxynitrile lyase. PhD Thesis, Technische Universität, Graz, Austria.

Bauer M, Griengl H, Steiner W. 1999. Kinetic studies on the enzyme (*S*)-hydroxynitrile lyase from *Hevea brasiliensis* using initial rate methods and progress curve analysis. *Biotechnol Bioeng 62*:20–29.

Bhat TN. 1988. Calculation of an OMIT map. *J Appl Crystallogr 21*:279–281.

Bhat TN, Cohen GH. 1984. OMITMAP: An electron density map suitable for the examination of errors in a macromolecular model. *J Appl Crystallogr 17*:244–248.

Brünger AT. 1992a. The free *R*-value: A novel statistical quantity for assessing the accuracy of crystal structures. *Nature 355*:472–474.

Brünger AT. 1992b. *X-PLOR, A system for X-ray crystallography and NMR*, Version 3.2. New Haven, Connecticut: Yale University Press.

Bürgi HB, Dunitz JD, Shefter E. 1973. Geometrical reaction coordinates. Nucleophilic addition to a carbonyl group. *J Am Chem Soc 95*:5065–5067.

CCP4 (Collaborative Computing Project, Number 4). 1994. The CCP4 suite—Programs for protein crystallography. *Acta Crystallogr D50*:760–763.

Conn EE. 1981. Secondary plant products. In: Stumpf PK, Conn EE, eds. *The biochemistry of plants: A comprehensive treatise*. New York: Academic Press.

Cygler M, Schrag JD, Sussman JL, Harel M, Silman I, Gentry MK, Doctor BP. 1993. Relationship between sequence conservation and three-dimensional structure in a large family of esterases, lipases, and related proteins. *Protein Sci 2*:366–382.

Effenberger F. 1994. Synthesis and reactions of optically-active cyanohydrins. *Angew Chem Int Ed Engl 33*:1555–1564.

Grochulski P, Li Y, Schrag JD, Bouthillier F, Smith P, Harrison D, Rubin B, Cygler M. 1993. Insights into interfacial activation from an open structure of *Candida rugoas* lipase. *J Biol Chem 268*:12843–12847.

Grochulski P, Li Y, Schrag JD, Cygler M. 1994. Two conformational states of *Candida rugosa* lipase. *Protein Sci 3*:82–91.

Gruber K, Klintschar G, Hayn M, Schlacher A, Steiner W, Kratky C. 1998. Thermophilic xylanase from *Thermomyces lanuginosus*: High-resolution X-ray structure and modelling studies. *Biochemistry 37*:13475–13485.

Gugganig M. 1997. Structure and kinetics of the hydroxynitrile lyase from *Hevea brasiliensis*. Diploma Thesis. Graz, Austria: Karl-Franzens-Universität.

Hasslacher M, Kratky C, Griengl H, Schwab H, Kohlwein SD. 1997a. Hydroxynitrile lyase from *Hevea brasiliensis*: Molecular characterization and mechanism of enzyme catalysis. *Proteins Struct Funct Genet 27*:438–449.

Hasslacher M, Schall M, Hayn M, Bona R, Rumbold K, Luckl J, Griengl H, Kohlwein SD, Schwab H. 1997b. High level intracellular expression of hydroxynitrile lyase from the tropical rubber tree *Hevea brasiliensis* in microbial hosts. *Protein Exp Purif 11*:61–71.

Hasslacher M, Schall M, Hayn M, Griengl H, Kohlwein SD, Schwab H. 1996a. Molecular cloning of the full-length cDNA of (*S*)-hydroxynitrile lyase from *Hevea brasiliensis*. Functional expression in *Escherichia coli* and *Saccharomyces cerevisiae* and identification of an active site residue. *J Biol Chem 271*:5884–5891.

Hasslacher M, Schall M, Hayn M, Griengl H, Kohlwein SD, Schwab H. 1996b. (*S*)-Hydroxynitrile lyase from *Hevea brasiliensis*. *Ann NY Acad Sci 799*: 707–712.

Hickel A, Hasslacher M, Griengl H. 1996. Hydroxynitrile lyases: Functions and properties. *Physiol Plant 98*:891–898.

Hughes J, Carvalho FJPDC, Hughes MA. 1994. Purification, characterization, and cloning of α-hydroxynitrile lyase from cassava (*Manihot esculenta* Crantz). *Arch Biochem Biophys 311*:496–502.

Johnson DV, Griengl H. 1997. The chemoenzymatic synthesis of (*S*) 13-hydroxyoctadeca-(9z,11e)-dienoic acid using the hydroxynitrile lyase from *Hevea brasiliensis*. *Tetrahedron 53*:617–624.

Johnson DV, Griengl H. 1999. Biocatalytic applications of hydroxynitrile lyases. *Adv Biochem Eng Biotechnol 63*:31–55.

Jones TA, Zou JY, Cowan S, Kjeldgaard M. 1991. Improved methods for building protein models in electron density maps and the location of errors in these models. *Acta Crystallogr A47*:110–119.

Klempier N, Griengl H, Hayn M. 1993. Aliphatic (*S*)-cyanhydrins by enzyme catalysed synthesis. *Tetrahedron Lett 34*:4769–4772.

Klempier N, Pichler U, Griengl H. 1995. Synthesis of α,β-unsaturated (*S*)-cyanohydrins using the oxynitrilase from *Hevea brasiliensis*. *Tetrahedron Asym 6*:845–848.

Kraulis PJ. 1991. MOLSCRIPT: A program to produce both detailed and schematic plots of protein structures. *J Appl Crystallogr 24*:946–950.

Kruse CG. 1992. Chiral cyanhydrins—Their manufacture and utility as chiral building blocks. In: Collins AN, Sheldrake GN, Crosby J, eds. *Chirality in industry*. London: John Wiley and Sons Ltd.

Kuroki GW, Conn EE. 1989. Mandelonitrile lyase from *Ximenia americana* L.: Stereospecificity and lack of flavin prosthetic group. *Proc Natl Acad Sci USA 86*:6978–6981.

Laskowski RA, MacArthur MW, Moss DS, Thornton JM. 1993. PROCHECK version 2.0. Programs to check the stereochemical quality of protein structures. *J Appl Crystallogr 26*:283–291.

Menard R, Khouri HE, Plouffe C, Dupras R, Ripoll D, Vernet T, Tessier DC, Laliberte F, Thomas DY, Storer AC. 1990. A protein engineering study of the role of aspartate 158 in the catalytic mechanism of papain. *Biochemistry 29*:6706–6713.

Merritt EA, Bacon DJ. 1997. Raster3D: Photorealistic molecular graphics. *Methods Enzymol 277*:505–524.

Ollis DL, Cheah E, Cygler M, Dijkstra B, Frolow F, Franken SM, Harel M, Remington SJ, Silman I, Schrag J, Sussman JL, Verschueren KHG, Goldman A. 1992. The α/β hydrolase fold. *Protein Eng 5*:197–211.

Otwinowski Z. 1990. DENZO data processing package. New Haven, Connecticut: Yale University Press.

Prelog V. 1964. Specification of the stereospecificity of some oxido-reductases by diamond lattice sections. *Pure Appl Chem 9*:119–130.

Quinn DM, Feaster SR. 1998. Esterases and lipases. In: Sinnott M, ed. *Comprehensive biological catalysis*. London: Academic Press.

Read RJ. 1986. Improved Fourier coefficients for maps using phases from partial structures with errors. *Acta Crystallogr A42*:140–149.

Schall M. 1996. Isolation and characterization of a (*S*)-hydroxynitrile lyase from *Hevea brasiliensis*. PhD Thesis. Graz, Austria: Karl Franzens Universität Graz.

Schmidt A, Gübitz GM, Kratky C. 1999. Xylan binding subsite mapping in the xylanase from *Penicillium simplicissimum* using xylooligosaccharides as cryo-protectant. *Biochemistry 38*:2403–2412.

Schmidt A, Schlacher A, Steiner W, Schwab H, Kratky C. 1998. Structure of the xylanase from *Penicillium simplicissimum*. *Protein Sci 7*:2081–2088.

Schrag JD, Cygler M. 1993. 1.8-Angstrom refined structure of the lipase from *Geotrichum candidum*. *J Mol Biol 230*:575–591.

Sheldrick GM. 1997. *SHELXL-97, A program for the refinement of crystal structures from diffraction data*. Göttingen, Germany: University of Göttingen.

Vellieux FMD, Dijkstra BW. 1997. Computation of Bhat's OMIT maps with different coefficients. *J Appl Crystallogr 30*:396–399.

Wagner UG, Hasslacher M, Griengl H, Schwab H, Kratky C. 1996. Mechanism of cyanogenesis: The crystal structure of hydroxynitrile lyase from *Hevea brasiliensis*. *Structure 4*:811–822.

Wajant H, Effenberger F. 1996. Hydroxynitrile lyases of higher plants. *Biol Chem 377*:611–617.

Wajant H, Mundry KW. 1993. Hydroxynitrile lyase from *Sorghum bicolor*: A glycoprotein heterotetramer. *Plant Sci 89*:127–133.

Wajant H, Pfizenmaier K. 1996. Identification of potential active-site residues in the hydroxynitrile lyase from *Manihot esculenta* by site-directed mutagenesis. *J Biol Chem 271*:25830–25834.

Wallace AC, Laskowski RA, Thornton JM. 1996. Derivation of 3D coordinate templates for searching structural databases—Application to Ser-His-Asp catalytic triads in the serine proteinases and lipases. *Protein Sci 5*:1001–1013.

Wharton CW. 1998. The serine proteinases. In: Sinnott M, ed. *Comprehensive biological catalysis*. London: Academic Press.

Xu L-L, Singh BK, Conn EE. 1988. Purification and characterization of acetone cyanhydrin lyase from *Linum usitatissimum*. *Arch Biochem Biophys 263*:256–263.